

pubs.acs.org/JPCL Letter

# Monitoring the Molecular Structure of Fibrinogen during the Adsorption Process at the Buried Silicone Oil Interface In Situ in Real Time

Tieyi Lu and Zhan Chen\*



Cite This: J. Phys. Chem. Lett. 2023, 14, 3139-3145



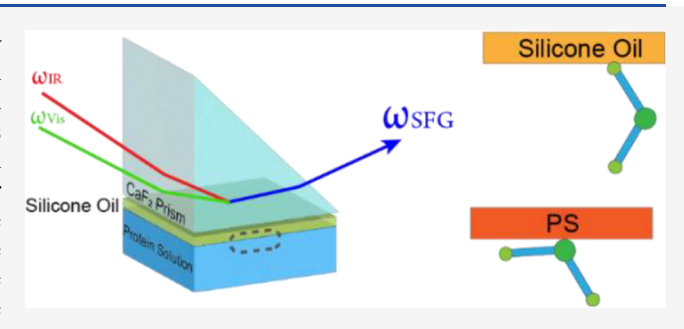
ACCESS I

III Metrics & More

Article Recommendations

s Supporting Information

ABSTRACT: Interfacial proteins play important roles in many research fields and applications, such as biosensors, biomedical implants, nonfouling coatings, etc. Directly probing interfacial protein behavior at buried solid/liquid and liquid/liquid interfaces is challenging. We used sum frequency generation vibrational spectroscopy and a Hamiltonian data analysis method to monitor the molecular structure of fibrinogen on silicone oil during the adsorption process in situ in real time. The results showed that the adsorbed fibrinogen molecules tend to adopt a bent structure throughout the entire adsorption process with the same orientation. This is different from the case of adsorbed fibrinogen



on CaF2 with a linear structure or on polystyrene with a bent structure but a different orientation. The method introduced herein is generally applicable for following time-dependent molecular structures of many other proteins and peptides at interfaces in situ in real time at the molecular level.

 $^{
m 7}$ he adsorption of a protein to a surface may have a negative impact. For example, it is the first event that occurs when a biomedical implant is placed into contact with tissue or blood. 1,2 Unfavorable protein-implant interactions may lead to undesirable biological responses such as blood coagulation, unnecessary immune responses, etc.<sup>3</sup> Also, the first step for marine biofouling on a ship is the adsorption of adhesive proteins generated by marine organisms to the ship hull. 4-6 Therefore, it is important to investigate the adsorption of protein to various surfaces to understand protein-surface interaction mechanisms for (1) the rational design of surfaces to prevent protein adsorption and/or (2) ensuring adsorbed proteins adopt "reasonable" structures that do not have an adverse effect. Protein adsorption has been extensively studied with a variety of characterization techniques, and excellent results have been obtained.7-11 However, almost all of the previously applied techniques have some limitations; thus, directly monitoring the adsorption process of the proteins at a buried solid/liquid or liquid/liquid interface in situ in real time with detailed molecular level protein structural information is still challenging.

In recent years, sum frequency generation (SFG) vibrational spectroscopy has been developed into a powerful tool for studying interfacial protein structure in situ. 9,12-39 SFG is a second-order nonlinear optical spectroscopic technique that can detect vibrational spectra of molecules on surfaces or at buried interfaces. Due to the selection rule of a second-order nonlinear optical process, only a medium without inversion

symmetry can generate an SFG signal under the electric-dipole approximation, making SFG a technique that is highly sensitive to the surface and/or interface.<sup>40–46</sup> Our previous studies demonstrated the successful application of SFG in examining the interfacial behavior of many proteins, such as physically adsorbed proteins on polymers, oils, and 2D materials, chemically immobilized enzymes on self-assembled monolayers and polymers, and membrane proteins associated with model cell membranes. 15-19,21-2

In this study, we applied SFG to follow the adsorption behavior of fibrinogen adsorbed to silicone oil at buried silicone oil/protein solution interface in situ in real time. Fibrinogen adsorption has been a focus for many protein adsorption studies due to its critical role in blood clot formation. Undesired adsorption and aggregation of fibrinogen may cause blood clot formation in a deep vein, called deep vein thrombosis.<sup>47</sup> The thromboembolism can cause serious outcomes if left unattended, 48 and it has become so common that it is considered an epidemic. 49,50 Understanding the adsorption of fibrinogen to surfaces with related structural changes in the adsorption process is an important step in

Received: February 3, 2023 Accepted: March 20, 2023 Published: March 24, 2023





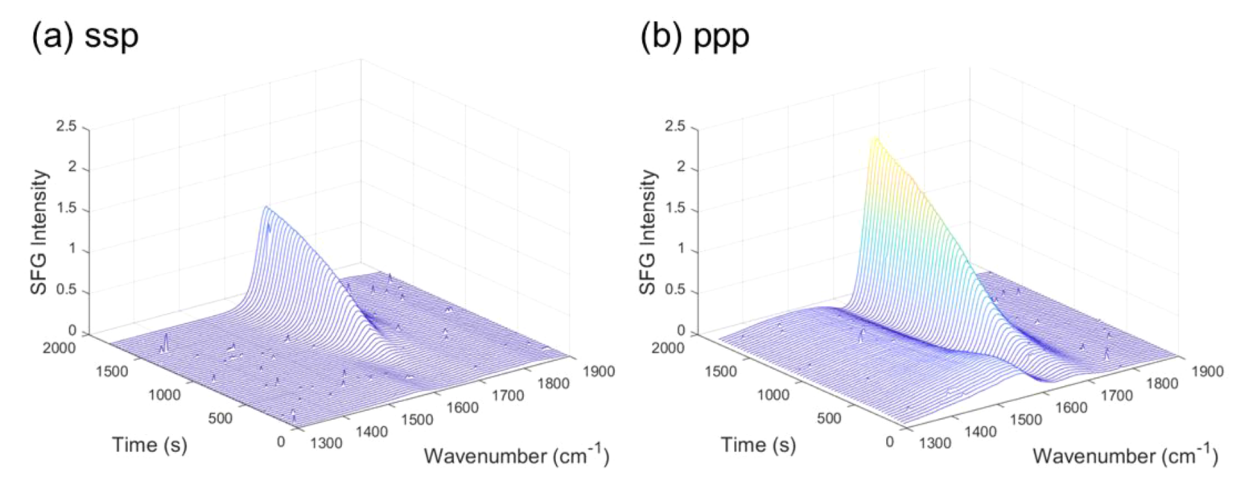


Figure 1. SFG (a) ssp and (b) ppp spectra collected from the silicone oil/fibrinogen solution (0.1 mg/mL) interface to follow the adsorption of fibrinogen to the silicone oil surface. The exposure time for each spectrum is 30 s. The fibrinogen solution was placed into contact with silicone oil at time zero. The spectra were recorded using a femtosecond SFG system. The spectral resolution is  $\sim$ 10 cm<sup>-1</sup>.

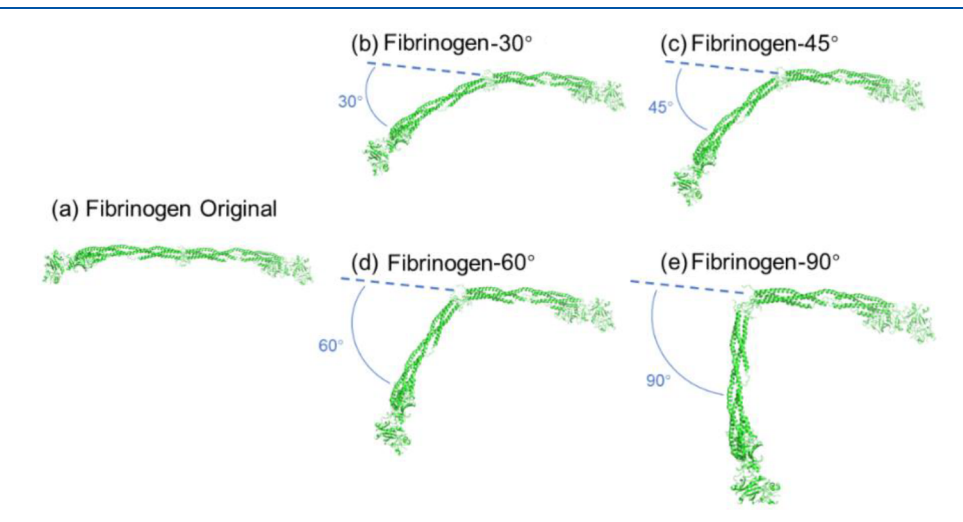


Figure 2. Structures of fibrinogen that were used for the Hamiltonian method in this study. (a) Original fibrinogen structure (PDB entry 3ghg). Half of the protein structure (chains A–C) was rotated by (b)  $30^{\circ}$ , (c)  $45^{\circ}$ , (d)  $60^{\circ}$ , or (e)  $90^{\circ}$  to approximate the possible bent conformations of fibrinogen.

unveiling the interfacial interaction and aggregation mechanism of fibrinogen, providing a basis for developing better thrombolytic therapies in the future. Silicone oil was chosen in this study as a surface for protein adsorption due to its strong hydrophobicity and wide application as the lubricant in the pharmaceutical industry. For protein drug (e.g., antibody drug) storage and administration, silicone oil is extensively used as a coating for a drug container or injector (e.g., a syringe).<sup>51</sup> It has been shown that the silicone oil coating can induce protein adsorption and possible aggregation, reducing antibody drug effectiveness. 52-54 In this study, we examined the dynamics of adsorption of fibrinogen to silicone oil in situ and in real time at the molecular level, elucidating the time-dependent fibringen structure in the adsorption process. The research results will be discussed below, and details about sample preparation, SFG experiments, and the Hamiltonian data analysis method<sup>55,56</sup> are presented in the Supporting Information.

The time-dependent SFG ssp and ppp spectra collected from the silicone oil/fibrinogen solution interface are shown in Figure 1. No discernible SFG protein amide I signal could be

detected from the silicone oil surface before the fibrinogen solution contact. After the fibrinogen solution was placed into contact with silicone oil, for the first 300 s, the SFG signal did not change substantially, indicating that the adsorption was slow during the initial adsorption process. After 300 s, the SFG amide I signals gradually became stronger and could be seen clearly. The peak at ~1645 cm<sup>-1</sup> in both ssp and ppp spectra can be attributed to the helical structure in fibrinogen. The SFG signal increased as a function of time, which can be caused by more adsorbed fibrinogen molecules, the change in the adsorbed fibrinogen structure (conformation and orientation), or both.

We can determine the conformation and orientation of adsorbed fibrinogen on silicone oil by comparing the calculated SFG spectra using the Hamiltonian method and the experimental data. Details of the Hamiltonian method are presented in section S1 of the Supporting Information. For comparison, it is necessary to remove the nonresonant contribution from the experimental data. Here the experimentally collected SFG spectra were fitted by the standard SFG spectral fitting method first (section S2 of the Supporting

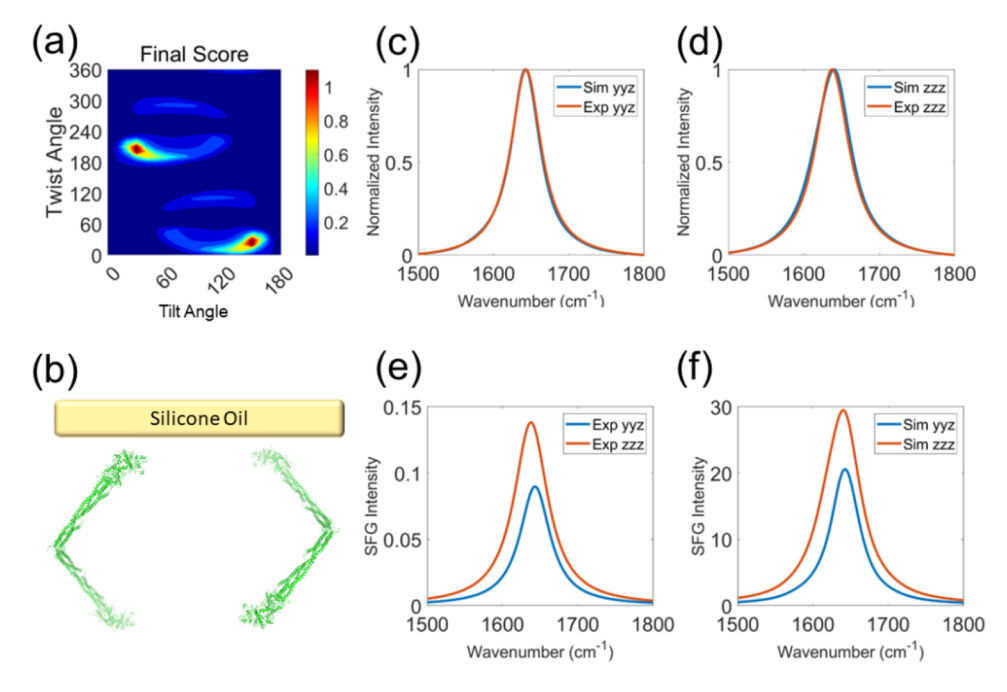


Figure 3. (a) Final matching score heat map showing the matching quality between the reconstructed resonant SFG experimental spectra (at 900 s) and the calculated orientation-dependent SFG spectra based on the fibrinogen-60° structure (shown in panel b). (b) Two most probable orientations of the adsorbed fibrinogen molecules on silicone oil. (c-f) Comparisons between reconstructed experimental data and calculated spectra based on the fibrinogen-60° structure with the highest matching score. The blue spectra in panels c and d are the calculated SFG yyz and zzz spectra, respectively, of adsorbed fibrinogen after adsorption for 900 s with the highest matching score with the reconstructed experimental resonant SFG spectra (orange). The unnormalized SFG spectra of (e) experimental data and (f) calculated spectra are plotted to evaluate the matching quality of the ssp and ppp spectral intensity ratio.

Information), <sup>57</sup> and then the resonant spectra were reconstructed using the fitting parameters (shown in Table S1). The ssp and ppp spectra can be converted to yyz and zzz spectra, respectively, by excluding the Fresnel coefficients (section S1 of the Supporting Information).

It is worth mentioning that when the Hamiltonian method is used to calculate SFG amide I signals from a protein, it considers the contributions from all of the peptide units in the protein. This method is advantageous compared to the previous method that considers only the contributions of the  $\alpha$ -helical components to the SFG amide I signals. The previous method needs to identify  $\alpha$ -helical components in a protein. The Hamiltonian method is more accurate for the calculation of SFG spectra.

The yyz and zzz SFG spectra of fibrinogen can be calculated as a function of fibrinogen molecular orientation using the Hamiltonian method based on a fibrinogen structure input. 55,56 In this study, the fibrinogen crystal structure [Proetin Data Bank (PDB) entry 3ghg, shown in Figure 2a] was used as a possible input structure for the Hamiltonian method. For the fibrinogen crystal structure, the two long coiled coils connect the two D domains with the center E domain, which can be treated as a long trinodal molecule. Our previous SFG results for the adsorption of fibrinogen to polystyrene, polyurethanes, and fluorinated polymers demonstrated that adsorbed fibrinogen molecules likely adopt bent structures, instead of the linear structure as shown in the crystal.

Here, to identify which conformation (linear or bent) fibrinogen adopts on the silicone oil surface, the original crystal structure (PDB entry 3ghg) was modified with different bent angles and these bent fibrinogen crystal structures were also

used as input structures for SFG spectral calculations with the Hamiltonian method. Specifically, we rotated chains A–C of the fibrinogen structure by 30°, 45°, 60°, and 90° to approximate the four bent conformations of fibrinogen. It is worth mentioning that this angle is not the bent angle between the two coiled coils in the molecule. All of the fibrinogen structures that were used for calculation in this study are shown in Figure 2. Note that these structures only served as the input structures for the SFG orientation analysis and the evaluation for possible fibrinogen conformational changes. They were not fully stabilized by simulation.

To probe the conformation and orientation of fibrinogen adsorbed to silicone oil as a function of time, the ssp (yyz) and ppp (zzz) spectra collected at 900, 1200, 1500, and 1800 s were compared with the calculated SFG spectra based on the five fibrinogen structures shown in Figure 2. No reliable fitting result can be obtained for the ssp spectra collected before 900 s due to the low signal intensity. For the SFG spectra collected at 900 s, upon comparison of the experimental and calculated spectra, the final match score heat map after considering the ssp and ppp spectra features and the ssp/ppp (yyz/zzz) spectra intensity ratio can be obtained for each of the five conformations with varied bent angles. It was found that the highest score in the matching score heat map obtained using the fibrinogen-60° structure (shown in Figure 2d) is higher than those of the other four heat maps (Table S2). Therefore, we believe that fibrinogen-60° is the most likely conformation adsorbed on the silicone oil at 900 s. According to the heat map shown in Figure 3a, the two most likely orientations are (tilt = 30, twist = 210) and (tilt = 150, twist = 30), shown in Figure 3b. These two orientations have the opposite absolution orientation. These two orientations are very similar, and we

believe that there is no need to differentiate between these two orientations.

To appreciate the similarity of the calculated spectra and the reconstructed experimental data with the highest matching score at 900 s, both the calculated spectra and the reconstructed experimental spectra are shown in Figure 3c–f. Panels c and d of Figure 3 show the matching qualities of the spectral features for the ssp and ppp spectra, respectively. Panels e and f of Figure 3 show the matching quality of the ssp/ppp spectral intensity ratio. Both the spectral features and the intensity ratio are well matched.

A method similar to that used to analyze the 900 s data can be used to analyze the SFG spectra collected at 1200, 1500, and 1800 s. The final matching score heat maps with the highest matching scores for each time are shown in Figures S4–S6, with the spectral comparisons between the calculated spectra and reconstructed experimental data with the highest matching scores. The highest matching scores of each fibrinogen conformation at each time step are listed in Table S2.

Table S2 shows that fibrinogen tends to adopt a bent structure rather than a linear structure throughout the entire adsorption process from 900 to 1800 s. Very similar matching score heat maps were obtained for fibrinogen adsorbed at different times, showing that the adsorbed fibrinogen orientation remains the same. Therefore, on a silicone oil surface, adsorbed fibrinogen does not change orientation or conformation as a function of time. This result is similar to what we observed from fibrinogen adsorbed on polystyrene, where fibrinogen adopted a bent structure. 16 However, this is different from what we observed for the adsorption of fibrinogen on polyurethane, fluorinated polymer, and silicone polymer surfaces previously, where time-dependent structural changes were detected. 9,58 Perhaps the liquid silicone oil surface is similar to the hydrophobic polystyrene surface; therefore, it is necessary for the adsorbed fibrinogen molecule to adopt a bent conformation. Also because of the flexible interface, it is easier to reach structural stability without having slow time-dependent structural changes.

In the past, we deduced the possible orientation of adsorbed fibrinogen on polystyrene based on the orientation of a single-helix structure. Here we reanalyzed the published SFG data using the Hamiltonian method and found that the calculated spectra based on fibrinogen-30° match the reconstructed experimental spectra best. Therefore, fibrinogen adsorbed on polystyrene adopts a bent structure. Its most likely orientation was deduced from the score heat map, as shown in Figure 4a.

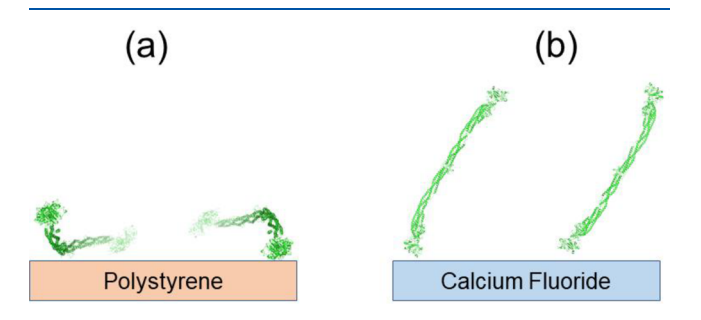
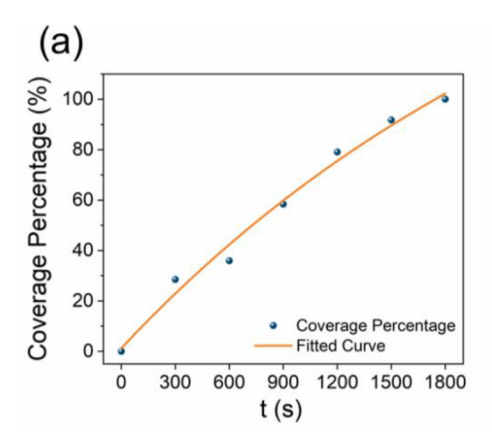


Figure 4. Deduced most likely conformation and orientation of adsorbed fibrinogen on (a) polystyrene and (b)  $CaF_2$ . The two orientations in each case have opposite absolute orientations, which cannot be distinguished by regular SFG results.

The detailed data analysis and related results of adsorbed fibrinogen on polystyrene are presented in section S4 of the Supporting Information. We believe that the left orientation shown in Figure 4a is the more likely orientation among the two opposite absolute orientations because it is more stable due to a larger area of contact with the surface. For comparison, we also analyzed our previously collected SFG spectra from fibrinogen adsorbed on CaF2. 15 Figure 4b shows the deduced most likely conformation and orientation of adsorbed fibrinogen on CaF2 using the Hamiltonian method (see details in section S5 of the Supporting Information). On CaF2, fibrinogen adopts a linear structure with a standing up orientation. The two structures shown in Figure 4b are similar, and thus, it is unnecessary to differentiate them. The interactions between the fibrinogen molecule and different surfaces such as hydrophobic and electrostatic interactions depend on the physicochemical properties of the surfaces. Silicone oil is a hydrophobic surface that favorably interacts with the hydrophobic domains of the fibrinogen strongly, causing a change in the fibrinogen conformation to a bent structure. The silicone oil is also very mobile; perhaps the silicone oil-fibrinogen interaction fluctuates, leading to a standing up pose for fibrinogen. Polystyrene is a hydrophobic surface with a negative charge, and the orientation and conformation of fibrinogen on polystyrene can be affected by the hydrophobic and electrostatic interactions together. The stronger interaction with the surface can possibly lead to a bent structure and a lying down orientation of half of the molecule. The CaF<sub>2</sub> surface is relatively hydrophilic, with weaker interactions with fibrinogen. Thus, fibrinogen adopts a native linear structure on the CaF2 surface. Overall, the conformation and orientation of fibrinogen on different surfaces are determined by various factors, such as the hydrophobicity of surfaces, electrostatic interaction, and the local chemistry environment. 59-61

The SFG intensity detected form adsorbed fibrinogen is related to the surface coverage and conformation and/or orientation. Because the conformation and orientation of adsorbed fibrinogen at 900, 1200, 1500, and 1900 s remain the same, we could deduce the time-dependent surface coverage of fibrinogen using the ppp SFG spectra (same as the ssp spectra). For shorter adsorption times of 300 and 600 s, although ssp SFG spectra cannot be reliably fitted, it is more feasible to fit the ppp SFG spectra (section S6 of the Supporting Information).

Here we use the adsorption at 1800 s as 100%. This does not mean that at 1800 s the adsorption is saturated or equilibrated. The 100% value at 1800 s here is just used as a standard to determine the relative surface coverages of fibrinogen at other time points. The trend in the deduced fibrinogen surface coverage percentage plot displayed in Figure 5 clearly indicates that the number of adsorbed fibrinogen molecules on silicone oil increases as a function of time and slowly approaches equilibrium. Figure 5 shows that at 1800 s, the fibrinogen surface coverage still continuously increases. The fitted curve on a longer time scale displayed in Figure 5 indicates that the fibrinogen adsorption reaches equilibrium at ~20000 s. The kinetics of fibrinogen adsorption may be influenced by both the adsorption/desorption balance at the interfaces and the diffusion of fibrinogen from the bulk to the interface. Our adsorption experiment was conducted using a static solution, which takes some time for the protein to diffuse to the interface. It will be interesting to compare the fibrinogen



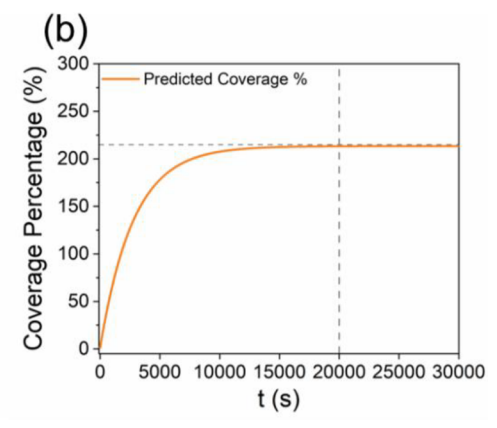


**Figure 5.** (a) Coverage percentage of fibrinogen on the silicone oil surface during adsorption. Black dots for experimental data and a red line for the fitting results. The date were fitted using the equation  $y = A \exp(x/t_0) + y_0$ , where y is the coverage and x is the time. The fitting results are as follows:  $y_0 = 213.4$ , A = 212.2, and  $t_0 = 2785$ . (b) Fitting curve on a longer time scale. This panel shows that the adsorption reaches equilibrium at  $\sim 20000$  s.

adsorption kinetics to that of a protein solution with a stirrer in the solution to minimize the diffusion process or a flow protein solution system, which is beyond the scope of this research.

In summary, the orientation and conformation of fibrinogen during the interfacial adsorption process have been deduced in situ in real time by SFG, with the help of a Hamiltonian SFG data analysis method. At the silicone oil/fibrinogen solution interface, the amount of fibrinogen adsorbed increases as a function of time, and the adsorption kinetics can be monitored in real time with SFG. More importantly, it was found that fibrinogen molecules adopt the same bent conformation and orientation during the adsorption process. The adsorbed bent fibrinogen molecules on the silicone oil surface are different from those on a CaF<sub>2</sub> surface or a polystyrene surface. Such similar or different conformations and orientations of fibrinogen on various surfaces can be further interpreted using computer simulations, which are beyond the scope of this research.

It is well known that fibrinogen adsorption is related to platelet adhesion and blood coagulation. However, the amount of fibrinogen adsorbed on a surface is not related to the amount of later adhered platelet, because the specific interaction between some small adhesive peptide regions of fibrinogen and the GPIIb/IIIa integrin receptor on platelets determines platelet adhesion. Therefore, the different adsorbed fibrinogen structures on various surfaces lead to varied platelet adhesion and blood coagulation effects.

This study successfully elucidated the molecular structure, including the conformation and orientation, of fibrinogen using an in situ SFG study. The fibrinogen molecular structure was monitored in real time, and the adsorption amount was deduced at the same time. Different conformations and orientations of fibrinogen on varied surfaces were observed. In the future, direct correlations between the adsorbed fibrinogen structure and platelet adhesion as well as the effect of blood coagulation on different surfaces could be investigated, providing in-depth understanding of the blood compatibility of many biomedical materials. The method developed in this research is general, which can be applied to study the adsorption process of many proteins in situ in real time at the molecular level.

#### ASSOCIATED CONTENT

### **Supporting Information**

The Supporting Information is available free of charge at https://pubs.acs.org/doi/10.1021/acs.jpclett.3c00331.

Experimental details, SFG instrument and sample geometry, fitting parameters, heat maps and matching quality comparison with different fibrinogen input structures, details of data analysis of SFG spectra collected from fibrinogen on polystyrene and CaF<sub>2</sub>, and details of the calculation of the coverage analysis (PDF)

## AUTHOR INFORMATION

#### **Corresponding Author**

Zhan Chen — Department of Chemistry, University of Michigan, Ann Arbor, Michigan 48109, United States; orcid.org/0000-0001-8687-8348; Email: zhanc@umich.edu

#### **Author**

Tieyi Lu — Department of Chemistry, University of Michigan, Ann Arbor, Michigan 48109, United States; orcid.org/ 0000-0003-0135-7653

Complete contact information is available at: https://pubs.acs.org/10.1021/acs.jpclett.3c00331

#### Notes

The authors declare no competing financial interest.

#### ACKNOWLEDGMENTS

This research is supported by the University of Michigan and the National Science Foundation (CHE-1904380). This work was performed in part at the University of Michigan Lurie Nanofabrication Facility.

#### REFERENCES

- (1) Bajpai, A. Fibrinogen adsorption onto macroporous polymeric surfaces: correlation with biocompatibility aspects. *J. Mater. Sci. Mater. Med.* **2008**, *19* (1), 343–357.
- (2) Horbett, T. A. Biological activity of adsorbed proteins. *Surfactant Sci. Ser.* **2003**, *110*, 393–413.
- (3) Castner, D. G.; Ratner, B. D. Biomedical surface science: Foundations to frontiers. *Surf. Sci.* **2002**, *500* (1–3), 28–60.

- (4) Amara, I.; Miled, W.; Slama, R. B.; Ladhari, N. Antifouling processes and toxicity effects of antifouling paints on marine environment. A review. *Environ. Toxicol. Pharmacol.* **2018**, *57*, 115–130.
- (5) Chen, S.; Li, L.; Zhao, C.; Zheng, J. Surface hydration: Principles and applications toward low-fouling/nonfouling biomaterials. *Polymer* **2010**, *51* (23), 5283–5293.
- (6) Wang, H.; Christiansen, D. E.; Mehraeen, S.; Cheng, G. Winning the fight against biofilms: the first six-month study showing no biofilm formation on zwitterionic polyurethanes. *Chem. Sci.* **2020**, *11* (18), 4709–4721.
- (7) Lu, J. Neutron reflection study of globular protein adsorption at planar interfaces. *Annu. Rep. Prog. Chem., Sect. C: Phys. Chem.* **1999**, 95, 3–46.
- (8) Wang, X.; Wang, Y.; Xu, H.; Shan, H.; Lu, J. R. Dynamic adsorption of monoclonal antibody layers on hydrophilic silica surface: A combined study by spectroscopic ellipsometry and AFM. *J. Colloid Interface Sci.* **2008**, 323 (1), 18–25.
- (9) Clarke, M. L.; Wang, J.; Chen, Z. Conformational changes of fibrinogen after adsorption. *J. Phys. Chem. B* **2005**, *109* (46), 22027–22035.
- (10) Green, R.; Davies, J.; Davies, M.; Roberts, C.; Tendler, S. Surface plasmon resonance for real time in situ analysis of protein adsorption to polymer surfaces. *Biomaterials* **1997**, *18* (5), 405–413.
- (11) Glassford, S. E.; Byrne, B.; Kazarian, S. G. Recent applications of ATR FTIR spectroscopy and imaging to proteins. *Biochim. Biophys. Acta Proteins Proteom.* **2013**, *1834* (12), 2849–2858.
- (12) Wang, J.; Even, M. A.; Chen, X.; Schmaier, A. H.; Waite, J. H.; Chen, Z. Detection of amide I signals of interfacial proteins in situ using SFG. J. Am. Chem. Soc. 2003, 125 (33), 9914–9915.
- (13) Wang, J.; Chen, X.; Clarke, M. L.; Chen, Z. Detection of chiral sum frequency generation vibrational spectra of proteins and peptides at interfaces in situ. *Proc. Natl. Acad. Sci. U.S.A.* **2005**, *102* (14), 4978–4983
- (14) Wang, J.; Clarke, M. L.; Chen, X.; Even, M. A.; Johnson, W. C.; Chen, Z. Molecular studies on protein conformations at polymer/liquid interfaces using sum frequency generation vibrational spectroscopy. *Surf. Sci.* **2005**, 587 (1–2), 1–11.
- (15) Wang, J.; Chen, X.; Clarke, M. L.; Chen, Z. Vibrational spectroscopic studies on fibrinogen adsorption at polystyrene/protein solution interfaces: hydrophobic side chain and secondary structure changes. *J. Phys. Chem. B* **2006**, *110* (10), 5017–5024.
- (16) Wang, J.; Lee, S.-H.; Chen, Z. Quantifying the ordering of adsorbed proteins in situ. J. Phys. Chem. B 2008, 112 (7), 2281–2290.
- (17) Nguyen, K. T.; Le Clair, S. V.; Ye, S.; Chen, Z. Orientation determination of protein helical secondary structures using linear and nonlinear vibrational spectroscopy. *J. Phys. Chem. B* **2009**, *113* (36), 12169–12180.
- (18) Ye, S.; Nguyen, K. T.; Le Clair, S. V.; Chen, Z. In situ molecular level studies on membrane related peptides and proteins in real time using sum frequency generation vibrational spectroscopy. *J. Struct. Biol.* **2009**, *168* (1), 61–77.
- (19) Boughton, A. P.; Yang, P.; Tesmer, V. M.; Ding, B.; Tesmer, J. J.; Chen, Z. Heterotrimeric G protein  $\beta1\gamma2$  subunits change orientation upon complex formation with G protein-coupled receptor kinase 2 (GRK2) on a model membrane. *Proc. Natl. Acad. Sci. U. S. A.* **2011**, *108* (37), E667–E673.
- (20) Ding, B.; Jasensky, J.; Li, Y.; Chen, Z. Engineering and characterization of peptides and proteins at surfaces and interfaces: a case study in surface-sensitive vibrational spectroscopy. *Acc. Chem. Res.* **2016**, 49 (6), 1149–1157.
- (21) Zou, X.; Wei, S.; Jasensky, J.; Xiao, M.; Wang, Q.; Brooks, C. L., III; Chen, Z. Molecular interactions between graphene and biological molecules. *J. Am. Chem. Soc.* **2017**, *139* (5), 1928–1936.
- (22) Li, Y.; Pan, D.; Nashine, V.; Deshmukh, S.; Vig, B.; Chen, Z. Understanding Protein-Interface Interactions of a Fusion Protein at Silicone Oil-Water Interface Probed by Sum Frequency Generation Vibrational Spectroscopy. *J. Pharm. Sci.* **2018**, *107* (2), *682*–*689*.

- (23) Zou, X.; Wei, S.; Badieyan, S.; Schroeder, M.; Jasensky, J.; Brooks, C. L., III; Marsh, E. N. G.; Chen, Z. Investigating the effect of two-point surface attachment on enzyme stability and activity. *J. Am. Chem. Soc.* **2018**, *140* (48), *16560*–*16569*.
- (24) Perera, H. G.; Lu, T.; Fu, L.; Zhang, J.; Chen, Z. Probing the Interfacial Interactions of Monoclonal and Bispecific Antibodies at the Silicone Oil—Aqueous Solution Interface by Using Sum Frequency Generation Vibrational Spectroscopy. *Langmuir* **2019**, 35 (44), 14339—14347.
- (25) Wei, S.; Zou, X.; Tian, J.; Huang, H.; Guo, W.; Chen, Z. Control of protein conformation and orientation on graphene. *J. Am. Chem. Soc.* **2019**, *141* (51), 20335–20343.
- (26) Xiao, M.; Wei, S.; Chen, J.; Tian, J.; Brooks, C. L., III; Marsh, E. N. G.; Chen, Z. Molecular Mechanisms of Interactions between Monolayered Transition Metal Dichalcogenides and Biological Molecules. *J. Am. Chem. Soc.* **2019**, *141* (25), 9980–9988.
- (27) Zhang, C.; Gao, J.; Hankett, J.; Varanasi, P.; Borst, J.; Shirazi, Y.; Zhao, S.; Chen, Z. Corn Oil–Water Separation: Interactions of Proteins and Surfactants at Corn Oil/Water Interfaces. *Langmuir* **2020**, *36* (15), 4044–4054.
- (28) Guo, W.; Zou, X.; Jiang, H.; Koebke, K. J.; Hoarau, M.; Crisci, R.; Lu, T.; Wei, T.; Marsh, E. N. G.; Chen, Z. Molecular Structure of the Surface-Immobilized Super Uranyl Binding Protein. *J. Phys. Chem.* B **2021**, *125* (28), 7706–7716.
- (29) Lu, T.; Guo, W.; Datar, P. M.; Xin, Y.; Marsh, E. N. G.; Chen, Z. Probing protein aggregation at buried interfaces: distinguishing between adsorbed protein monomers, dimers, and a monomer–dimer mixture in situ. *Chem. Sci.* **2022**, *13* (4), 975–984.
- (30) Jung, S.-Y.; Lim, S.-M.; Albertorio, F.; Kim, G.; Gurau, M. C.; Yang, R. D.; Holden, M. A.; Cremer, P. S. The Vroman effect: a molecular level description of fibrinogen displacement. *J. Am. Chem. Soc.* 2003, 125 (42), 12782–12786.
- (31) Fu, L.; Wang, Z.; Yan, E. C. N-H Stretching Modes Around 3300 Wavenumber From Peptide Backbones Observed by Chiral Sum Frequency Generation Vibrational Spectroscopy. *Chirality* **2014**, *26* (9), 521–524.
- (32) Roy, S.; Covert, P. A.; FitzGerald, W. R.; Hore, D. K. Biomolecular structure at solid-liquid interfaces as revealed by nonlinear optical spectroscopy. *Chem. Rev.* **2014**, *114* (17), 8388–8415.
- (33) Ye, S.; Li, H.; Yang, W.; Luo, Y. Accurate determination of interfacial protein secondary structure by combining interfacial-sensitive amide I and amide III spectral signals. *J. Am. Chem. Soc.* **2014**, 136 (4), 1206–1209.
- (34) Huang, J.; Tian, K.; Ye, S.; Luo, Y. Amide III SFG Signals as a Sensitive Probe of Protein Folding at Cell Membrane Surface. *J. Phys. Chem. C* **2016**, *120* (28), 15322–15328.
- (35) Tan, J.; Zhang, J.; Luo, Y.; Ye, S. Misfolding of a human islet amyloid polypeptide at the lipid membrane populates through  $\beta$ -sheet conformers without involving  $\alpha$ -helical intermediates. *J. Am. Chem. Soc.* **2019**, *141* (5), 1941–1948.
- (36) Hosseinpour, S.; Roeters, S. J.; Bonn, M.; Peukert, W.; Woutersen, S.; Weidner, T. Structure and dynamics of interfacial peptides and proteins from vibrational sum-frequency generation spectroscopy. *Chem. Rev.* **2020**, *120* (7), 3420–3465.
- (37) Weidner, T.; Castner, D. G. Developments and Ongoing Challenges for Analysis of Surface-Bound Proteins. *Annu. Rev. Anal. Chem.* **2021**, *14*, 389–412.
- (38) Guo, W.; Lu, T.; Gandhi, Z.; Chen, Z. Probing orientations and conformations of peptides and proteins at buried interfaces. *J. Phys. Chem. Lett.* **2021**, *12* (41), 10144–10155.
- (39) Fu, L.; Liu, J.; Yan, E. C. Chiral sum frequency generation spectroscopy for characterizing protein secondary structures at interfaces. *J. Am. Chem. Soc.* **2011**, *133* (21), 8094–8097.
- (40) Shen, Y. Surface properties probed by second-harmonic and sum-frequency generation. *Nature* **1989**, 337 (6207), 519.
- (41) Zhuang, X.; Miranda, P.; Kim, D.; Shen, Y. Mapping molecular orientation and conformation at interfaces by surface nonlinear optics. *Phys. Rev. B* **1999**, *59* (19), 12632.

- (42) Moad, A. J.; Simpson, G. J. A unified treatment of selection rules and symmetry relations for sum-frequency and second harmonic spectroscopies. *J. Phys. Chem. B* **2004**, *108* (11), 3548–3562.
- (43) Khan, M. R.; Singh, H.; Sharma, S.; Asetre Cimatu, K. L. Direct Observation of Adsorption Morphologies of Cationic Surfactants at the Gold Metal—Liquid Interface. *J. Phys. Chem. Lett.* **2020**, *11* (22), 9901—9906.
- (44) Lukas, M.; Schwidetzky, R.; Kunert, A. T.; Backus, E. H.; Pöschl, U.; Fröhlich-Nowoisky, J.; Bonn, M.; Meister, K. Interfacial Water Ordering Is Insufficient to Explain Ice-Nucleating Protein Activity. *J. Phys. Chem. Lett.* **2021**, *12* (1), 218–223.
- (45) Rehl, B.; Gibbs, J. M. Role of ions on the surface-bound water structure at the silica/water interface: identifying the spectral signature of stability. *J. Phys. Chem. Lett.* **2021**, *12* (11), 2854–2864.
- (46) Luo, Y.; Pang, A.-P.; Zhu, P.; Wang, D.; Lu, X. Demonstrating the Interfacial Polymer Thermal Transition from Coil-to-Globule to Coil-to-Stretch under Shear Flow Using SFG and MD Simulation. *J. Phys. Chem. Lett.* **2022**, *13* (6), 1617–1627.
- (47) Kyrle, P. A.; Eichinger, S. Deep vein thrombosis. *Lancet* **2005**, 365 (9465), 1163–1174.
- (48) Collins, R.; Scrimgeour, A.; Yusuf, S.; Peto, R. Reduction in fatal pulmonary embolism and venous thrombosis by perioperative administration of subcutaneous heparin. *New Engl. J. Med.* **1988**, 318 (18), 1162–1173.
- (49) Lee, A. Y.; Levine, M. N.; Baker, R. I.; Bowden, C.; Kakkar, A. K.; Prins, M.; Rickles, F. R.; Julian, J. A.; Haley, S.; Kovacs, M. J.; Gent, M. Low-molecular-weight heparin versus a coumarin for the prevention of recurrent venous thromboembolism in patients with cancer. N. Engl. J. Med. 2003, 349 (2), 146–153.
- (50) Dowling, N.; Austin, H.; Dilley, A.; Whitsett, C.; Evatt, B.; Hooper, W. The epidemiology of venous thromboembolism in Caucasians and African-Americans: the GATE Study 1. *J. Thrombosis Haemostasis* **2003**, *1* (1), 80–87.
- (51) Kearns, V. R.; Williams, R. L. Drug delivery systems for the eye. Exp. Rev. Med. Devices 2009, 6 (3), 277–290.
- (52) Jones, L. S.; Kaufmann, A.; Middaugh, C. R. Silicone oil induced aggregation of proteins. J. Pharm. Sci. 2005, 94 (4), 918–927.
- (53) Thirumangalathu, R.; Krishnan, S.; Ricci, M. S.; Brems, D. N.; Randolph, T. W.; Carpenter, J. F. Silicone oil-and agitation-induced aggregation of a monoclonal antibody in aqueous solution. *J. Pharm. Sci.* **2009**, 98 (9), 3167–3181.
- (54) Gerhardt, A.; Bonam, K.; Bee, J. S.; Carpenter, J. F.; Randolph, T. W. Ionic strength affects tertiary structure and aggregation propensity of a monoclonal antibody adsorbed to silicone oil—water interfaces. *J. Pharm. Sci.* **2013**, *102* (2), 429–440.
- (55) Hamm, P.; Zanni, M. Concepts and Methods of 2D Infrared Spectroscopy; Cambridge University Press, 2011.
- (56) Ding, B.; Panahi, A.; Ho, J.-J.; Laaser, J. E.; Brooks, C. L., III; Zanni, M. T.; Chen, Z. Probing site-specific structural information of peptides at model membrane interface in situ. *J. Am. Chem. Soc.* **2015**, 137 (32), 10190–10198.
- (57) Chen, Z.; Shen, Y.; Somorjai, G. A. Studies of polymer surfaces by sum frequency generation vibrational spectroscopy. *Annu. Rev. Phys. Chem.* **2002**, *53* (1), 437–465.
- (58) Liu, Y.; Jasensky, J.; Chen, Z. Molecular interactions of proteins and peptides at interfaces studied by sum frequency generation vibrational spectroscopy. *Langmuir* **2012**, *28* (4), 2113–2121.
- (59) Sit, P. S.; Marchant, R. E. Surface-dependent conformations of human fibrinogen observed by atomic force microscopy under aqueous conditions. *Thrombosis Haemostasis* **1999**, 82 (09), 1053–1060.
- (60) Lin, Y.; Wang, J.; Wan, L.-J.; Fang, X.-H. Study of fibrinogen adsorption on self-assembled monolayers on Au (1 1 1) by atomic force microscopy. *Ultramicroscopy* **2005**, *105* (1–4), 129–136.
- (61) Dubrovin, E. V.; Barinov, N. A.; Schäffer, T. E.; Klinov, D. V. In situ single-molecule AFM investigation of surface-induced fibrinogen unfolding on graphite. *Langmuir* **2019**, *35* (30), *9732*–*9739*.
- (62) Horbett, T. A. Fibrinogen adsorption to biomaterials. J. Biomed. Mater. Res. Part A 2018, 106 (10), 2777–2788.

# ☐ Recommended by ACS

# Adsorption Kinetics of Type-III Antifreeze Protein on Ice Crystal Surfaces

Dmitry A. Vorontsov, Ekaterina L. Kim, et al.

JUNE 09, 2023

LANGMUIR

READ 🗹

## **Characterizing Interfaces by Voronoi Tessellation**

Daniel Konstantinovsky, Sharon Hammes-Schiffer, et al.

JUNE 02, 2023

THE JOURNAL OF PHYSICAL CHEMISTRY LETTERS

READ 🗹

# Investigating the Orientation of an Interfacially Adsorbed Monoclonal Antibody and Its Fragments Using Neutron Reflection

Sean Ruane, Jian R. Lu, et al.

FEBRUARY 16, 2023

MOLECULAR PHARMACEUTICS

READ 🗹

#### New Insights into Cation- and Temperature-Driven Protein Adsorption to the Air-Water Interface through Infrared Reflection Studies of Bovine Serum Albumin

Abigail A. Enders, Heather C. Allen, et al.

APRIL 07, 2023

LANGMUIR

READ 🗹

Get More Suggestions >